

K band spectroscopy of Herbig Ae/Be stars

M. Ishii (Subaru Telescope), M. Tamura (NAOJ), T. Nagata, S. Sato (Nagoya Univ.), Y. Yao, Z. Jiang (Purple Mountain Observatory), & K. Yanagisawa (Okayama Astrophysical Observatory).

1. Introduction

While the evolutionary status of low-mass young stars has been successfully classified by the spectral energy distributions (SEDs), such classification scheme has not been established for massive ($\gtrsim 2 M_{\odot}$) young stellar objects (YSOs). To solve the problem, near-infrared spectroscopy can be a powerful tool, revealing details about the physical natures of YSO photospheres and circumstellar environments (accretion disks, stellar winds, outflows, extinction, effective temperature, etc.). With this point of view, we observed the near-infrared *K* band spectra of 54 Herbig Ae/Be stars (HAeBes). They were selected from the list by Thé et al. (1994) to cover wide range of spectral type (from O7 to F3), stellar mass ($\sim 2\text{--}40 M_{\odot}$), age ($\sim 10^4\text{--}10^7$ yr), and SED.

2. Observations and Results

The 2.05 to 2.35 μm spectra were obtained with Super-OASIS mounted on the 1.88-m telescope at Okayama Astrophysical Observatory. The spectral resolution was $\lambda/\Delta\lambda \sim 500$ with a 2.4'' wide slit. As a result, Br γ (2.166 μm), He I (2.059 μm), Fe II (2.089 μm), He I (2.113 μm), H $_2$ (2.122 μm), Mg II (2.137/2.144 μm), Na I (2.206/2.209 μm), and CO (2.294 μm) were detected.

With these lines, *K* band spectra of HAeBe stars can be classified into 5 patterns (Figure 1): (1) those with only Br γ emission/absorption (35 objects), (2) those with He I 2.059 μm emission (including those with Fe II, Mg II, and He I 2.113 μm also) (9 objects), (3) those with CO bands in emission/absorption (also including those with Na I emission/absorption) (7 objects), (4) those with H $_2$ emission (1 object), and (5) those with no features (3 objects). All except for one (MWC 137) of our HAeBe sample belong to each one of the 5 categories (MWC 137 applies to two categories, 2 and 3).

These five categories depend on the spectral type, to some extent. Most (87%) of the Herbig Ae sample belong to the category (1) only Br γ or (5) no feature. On the other hand, Herbig Be stars are more likely to show a variety of features — 43% of them belong to the category (2) and/or (3), while 57% of them belong to the category (1) or (5).

2.1 Br γ emission

Br γ emission is most frequently observed in the *K* band spectra of HAeBe stars. The emission line

occurs in the ionized circumstellar region, although whether the emitting gas is part of the wind or part of an accretion stream is a matter of debate.

In Fig. 2*a*, observed equivalent widths (EWs) of Br γ ($EW_{Br\gamma,Obs}$) are plotted against the stellar effective temperature (T_{eff}). The figure shows the tendency for lower temperature stars to show weaker Br γ emission. On the other hand, because A-type stars show strong H I absorptions in the photosphere, $EW_{Br\gamma,Obs}$ of HAeBe stars could be the combination of the circumstellar emission and the photospheric absorption. In Fig. 2*b*, where the Br γ EWs corrected for the photospheric absorption ($EW_{Br\gamma,CS}$) are plotted, dispersion of the EW and its dependence on T_{eff} is smaller than that seen in Fig. 2*a*.

Corcoran & Ray (1998) showed that EW of H α emission of HAeBes correlates with near-infrared colors $H - K$ and $K - L$, which is regarded as a measure of accretion rate. On the other hand, we found no correlation between the Br γ EW and the excess circumstellar emission (Fig. 3). To clarify the problem, we plot the H α and Br γ EWs against $H - K$ for those HAeBe stars that were observed by Corcoran & Ray (1998) as well as by us (Fig. 4). The figure shows that $EW_{Br\gamma,Obs}$ (triangles) is not correlated with $H - K$, while the H α EW (squares) is well correlated with it. Thus, Br γ emission of HAeBe stars shows different behavior than H α emission.

From the correlation with NIR colors, H α EW could be regarded a rough measure of accretion activity of HAeBe stars. For T Tauri stars, on the other hand, Br γ line is a better indicator of accretion than H α that prone to have contribution from extended outflowing regions as well. If this could also apply to HAeBe stars, one would expect that Br γ shows better correlation with $H - K$ than H α . However we found the opposite results. Therefore we suspect either that NIR excess ($H - K$, K_{excess}) is poorly related with the accretion activity of HAeBe stars or that Br γ does not originate from an accretion flow.

In Fig. 5, $EW_{Br\gamma,CS}$ is plotted against the stellar age, with different symbols according to the stellar mass. With our HAeBe sample, stellar age distribution depends strongly on the stellar mass. When we consider early-type HAeBe stars (*open-symbols*) and late-type HAeBe stars (*filled-symbols*) separately, we found no correlation between Br γ EW and the stellar age. Because Br γ emission from HAeBe stars is thought to be a product of the accretion and/or outflow activities and such activities generally appear to decrease with time, one would expect a decreasing tendency of Br γ EW with increasing stellar age. However, we do

not find such a tendency in any stellar mass range.

2.2 Comparison with luminous Class I YSOs

We compared the K band spectra of HAeBe stars with those of Class I YSOs which are considered to be the precursors of them (Ishii et al. 2001). The detection rate and the EWs of $\text{Br}\gamma$ emission are similar between HAeBe stars and the Class I objects. On the other hand, the detection rate of the H_2 emission in the HAeBe sample is much lower than that found in the Class I YSOs. This indicates that the detection of H_2 emission is related to the degree of the dispersal of circumstellar envelopes, where H_2 molecules are

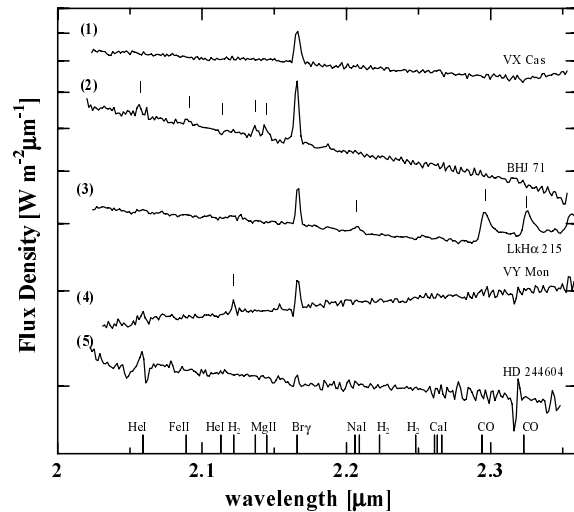


Figure 1: K band spectra of Herbig Ae/Be stars

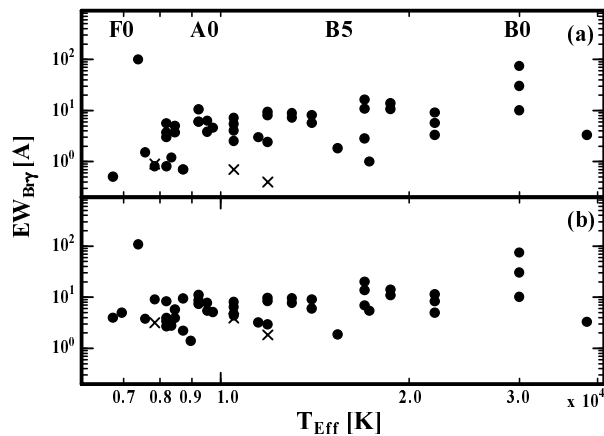


Figure 2: (a) Observed $\text{Br}\gamma$ equivalent widths (EWs) and (b) circumstellar $\text{Br}\gamma$ emission EWs of HAeBe stars are plotted against the effective temperature. Circles and crosses represent those with and without the $\text{Br}\gamma$ detection, respectively. In this and following figures, positive EW indicates emission features.

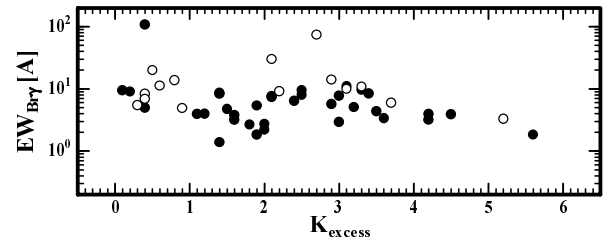


Figure 3: EWs of $\text{Br}\gamma$ emission of HAeBe stars are plotted against excess continuum emission at K ($K_{\text{excess}} = V - (V - K)_0 - 0.89A_V - K$). Open circles and filled circles represent $\geq 5M_{\odot}$ and $< 5M_{\odot}$ sources, respectively.

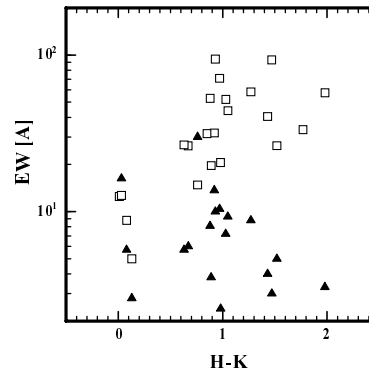


Figure 4: $\text{Br}\gamma$ EWs (*triangles*) and $\text{H}\alpha$ EWs (*squares*) of HAeBe stars vs. $(H - K)$. $\text{H}\alpha$ and $H - K$ data are taken from Corcoran & Ray (1998)

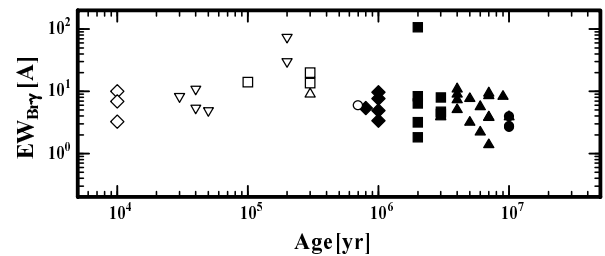


Figure 5: $\text{Br}\gamma$ EWs of HAeBe stars vs. stellar age. In this figure, HAeBe stars are classified according to the stellar mass: filled circles, filled triangles, filled squares, filled diamonds, open circles, open triangles, open squares, open inverted-triangles, and open diamonds represent $1 \leq M_{\star} < 2$, $2 \leq M_{\star} < 3$, $3 \leq M_{\star} < 4$, $4 \leq M_{\star} < 5$, $5 \leq M_{\star} < 6$, $6 \leq M_{\star} < 7$, $7 \leq M_{\star} < 10$, $10 \leq M_{\star} < 20$, and $20 \leq M_{\star}$, respectively.

References

Corcoran, M., & Ray, T. P. 1998, *A&A*, 331, 147
 Ishii, M., et al. 2001, *AJ*, 121, 3191
 Thé, P. S., et al. 1994, *A&AS*, 104, 315